

Monitoring autophagic flux in *Caenorhabditis elegans* using a p62/SQST-1 reporter

Christina Ploumi^{a,b}, Aggeliki Sotiriou^{a,b}, and Nektarios Tavernarakis^{a,b,*}

^a*Institute of Molecular Biology and Biotechnology, Foundation for Research and Technology-Hellas, Heraklion, Crete, Greece*

^b*Department of Basic Sciences, Faculty of Medicine, University of Crete, Heraklion, Crete, Greece*

*Corresponding author: e-mail address: tavernarakis@imbb.forth.gr

Chapter outline

1 Introduction	74
2 Materials	76
2.1 Disposables.....	76
2.2 Equipment.....	77
2.3 Reagents.....	77
2.4 Nematode strains.....	79
2.5 Nematode food.....	79
2.6 Microscopic analysis for monitoring autophagic flux using the SQST-1::GFP reporter strain.....	79
2.7 Detection of SQST-1::GFP levels by western blot.....	81
2.8 Notes.....	83
3 Concluding remarks	85
Acknowledgments	85
References	85

Abstract

Autophagy is a well-conserved self-degrading mechanism, which involves the elimination of unnecessary or damaged cellular constituents. Although extensively studied, many aspects regarding its tight regulation and its implication in health and disease remain elusive. The nematode *Caenorhabditis elegans* has been widely used as a simple multicellular model organism for studying the autophagic machinery per se, and uncover its multidimensional roles in the

maintenance of cellular and organismal homeostasis. The current protocol describes the *in vivo* detection and biochemical analysis of the autophagic substrate SQST-1, as an indicator of autophagic flux in *C. elegans*.

1 Introduction

Autophagy is a physiological, highly regulated process, which functions by eliminating superfluous or damaged cellular components. Canonical autophagy is generally classified into three main types: macroautophagy, microautophagy and chaperone-mediated autophagy. Macroautophagy is characterized by the formation of autophagosomes, double-membraned vesicles which engulf the cytoplasmic material. The resulted autophagosomes subsequently fuse with lysosomes, forming autolysosomes, in which the engulfed cytoplasmic cargo is finally degraded by lysosomal hydrolases (Feng et al., 2014). In microautophagy, the cytoplasmic components are directly taken up by the lysosome for degradation through invagination of the lysosomal membrane (Oku & Sakai, 2018). Finally, chaperone-mediated autophagy (CMA) involves the selective degradation of proteins containing KFERQ-related motifs. The particular motif is recognized by chaperone heatshock cognate 71 kDa (HSC70), which in turn delivers the protein to the lysosomes by interacting with the cytosolic tail of lysosome-associated membrane protein 2A (LAMP-2A) (Kaushik & Cuervo, 2018).

Macroautophagy (hereafter mentioned as autophagy), was initially described as a bulk, non-selective catabolic mechanism, triggered by unfavorable conditions, such as caloric restriction or starvation. However, it is now well established that autophagy is a highly selective and tightly regulated process that involves specialized receptors and adaptor proteins (Dikic & Elazar, 2018; Metaxakis, Ploumi, & Tavernarakis, 2018; Reggiori et al., 2012). Previous studies in yeast have identified more than 30 evolutionarily conserved autophagy-related genes (ATGs), essential for each step of the autophagic process: initiation, formation/nucleation of the autophagosomes, elongation, lysosomal fusion and degradation of the autophagosomal content. Autophagy is initiated by the activation and recruitment of the ULK1 complex [ULK1/Atg1, FIP200, ATG13 and ATG101] to the pre-autophagosomal membrane structures [Endoplasmic Reticulum (ER) or endosomal membranes]. ULK1 complex in turn activates Beclin 1, leading to the recruitment of VPS34 complex [Beclin 1, VPS34, VPS15, ATG14L], which acts as a Phosphoinositide 3-kinase (PI3K) to generate Phosphatidylinositol 3-phosphate (PI3P). Subsequently, PI3Ps bind to WD-repeat protein interacting with phosphoinositides (WIPI) proteins which recruit specific ATGs for the expansion and nucleation of the preautophagosomal membrane, known as the phagophore. The critical step at this point is the conjugation of LC3/Atg8 to PE lipids. This Ubiquitin-like reaction is orchestrated by the coordinated function of ATG7, ATG3 and ATG5-12-16, which act as E1, E2 and E3

enzymes, respectively. As phagophore membrane expands (elongation step), specific adaptor proteins, including P62/SQSTM1 (phosphotyrosine-independent ligand for the Lck SH2 domain of 62KDa/sequestosome) start to sequester ubiquitinated cytoplasmic constituents (i.e., aggregated proteins, organelles, etc.) through direct interaction with the lipidated form of LC3 (LC3-II). The loaded phagophore finally closes in an ATG2-dependent manner giving rise to the mature autophagosome. The autophagosome then fuses with a lysosome for the degradation of the engulfed cargo, a process dependent on microtubules and tethering factors, including soluble NSF attachment protein receptors (SNAREs) and homotypic fusion and protein sorting (HOPS) complexes (Dikic & Elazar, 2018; Feng et al., 2014; Metaxakis et al., 2018; Saha et al., 2018).

During the past two decades, preclinical and clinical studies have consistently highlighted the implication of autophagy in the pathogenesis of human diseases. Among others, deregulation of autophagy is associated with neurodegenerative disorders, autoimmune diseases, cardiomyopathies, inflammatory diseases and cancer, as well as accelerating ageing (Levine & Kroemer, 2008; Menzies et al., 2017; Metaxakis et al., 2018). Several steps of the autophagic process can be enhanced or blocked by specific drugs; therefore, pharmacological manipulation of autophagy for therapeutic purposes is a long-cherished goal. Indeed, numerous clinical trials are underway to explore the potential of well established and novel autophagy targeting drugs as therapeutic approaches for these diseases (Galluzzi et al., 2017; Levy, Towers, & Thorburn, 2017).

In parallel, animal models are used to delineate the molecular mechanisms that regulate this complicated catabolic pathway. Most ATG genes have a single ortholog in *Caenorhabditis elegans*, one of the simplest multicellular organisms, yet closely related to higher eukaryotes. *C. elegans* has been extensively used as a model to investigate the basic mechanisms of autophagy and understand its multifaceted roles in physiology and ageing (Markaki, Palikaras, & Tavernarakis, 2018; Tian et al., 2010). Furthermore, several disease models have been developed in *C. elegans*, making this tiny organism a remarkable tool to explore autophagy-targeting therapeutic approaches for neurodegeneration, cancer and other human disorders (Fang et al., 2019; Kyriakakis, Markaki, & Tavernarakis, 2015; Scott et al., 2017; Wong et al., 2020).

Previous studies have employed a variety of methodological approaches to monitor autophagy in *C. elegans* (Chen, Scarcelli, & Legouis, 2017; Klionsky et al., 2016; Papandreou & Tavernarakis, 2017; Zhang et al., 2015). These mainly include the expression analysis of core autophagic components both at the transcriptional and translational level, using *in vivo* imaging or western blotting. Furthermore, despite its small size and the thick collagenous cuticle covering its whole body, *C. elegans* has been also used as a sample for transmission electron microscopy (TEM), which allows the visualization of subcellular autophagic events in high magnification and resolution (Kovács, 2015). A fundamental and widespread approach for studying autophagy in nematodes involves the use of GFP::LGG-1 translational reporters. LGG-1 (LC3, GABARAP and GATE-16 family) is one of the two Atg8/LC3

orthologs in *C. elegans*, the lipidated form of which is associated with the autophagosomal membranes. Microscopic analysis of these reporters unravels the formation of highly dynamic puncta (representing autophagosomes), which are visible in almost all tissues throughout the animal's life, from embryonic, to larval and adult stages (Palmisano & Melendez, 2016a; Zhang et al., 2015). Increased number of LGG-1 puncta does not necessarily reflect autophagy induction, since autophagosomes may accumulate due to blockage of the autophagic flux. To ensure that the autophagic process is not blocked, it is highly recommended to monitor in parallel the degradation of well-characterized substrates that are degraded through autophagy. Apart from its role as an autophagy receptor and adaptor protein (i.e., mediating the interaction of ubiquitinated cytoplasmic cargoes with LGG-1/LC3), sequestosome (SQST-1)/p62 is a well-known autophagic substrate, which can be used for monitoring autophagic flux (Guo et al., 2014; Kumsta et al., 2019; Pankiv et al., 2007; Tian et al., 2010). Under autophagy inducing conditions, such as starvation, GFP::LGG-1 puncta are increased while SQST-1 puncta are reduced, since they are degraded through autophagy (Aspernig et al., 2019; Charnpilas et al., 2020; Feleciano et al., 2019; Pietrocola et al., 2018; Sharma, Pandey, & Saluja, 2018; Zhou et al., 2019). Inversely, upon conditions that block autophagy, both LGG-1 and SQST-1 puncta persist in various tissues, due to the inability of the autophagic machinery to complete the degradation of the autophagosomal cargo (Guerrero-Gomez et al., 2019; Kalfalah et al., 2016; Kim et al., 2018).

In the current protocol we describe the experimental procedure for monitoring autophagic flux in *C. elegans* young adults, using an SQST-1 reporter under both normal and autophagy inducing conditions (i.e., starvation). Particularly, we analyze how to visualize SQST-1 expression using *in vivo* imaging and how to biochemically detect SQST-1 levels through western blot analysis. For accurately monitoring autophagic flux, this method should always be combined with the expression analysis of GFP::LGG-1 reporters (Palmisano & Melendez, 2016a; Palmisano & Melendez, 2016b).

2 Materials

2.1 Disposables

1. Microscope slides (25.4 mm × 76.2 mm × 1 mm)
2. Microscope coverslips (18 mm × 18 mm)
3. Fingernail polish for sealing the coverslips
4. Standard platinum wire pick: for transferring the worms to NGM plates
5. Eyelash hair: for transferring the worms on agarose pads directly before observation in the microscope
6. Petri plates (60 × 15 mm) for the maintenance of *C. elegans* nematodes
7. Petri plates (92 × 16 mm) for bacterial growth
8. Agarose pads: Add 0.5 g agarose into 25 mL distilled H₂O. Heat the solution until the agarose is completely dissolved. While the agarose is still hot, leave a droplet (approximately 1 cm in diameter) in the middle of a microscope slide.

Immediately place a second slide on the top of it, and press it until the agarose droplet is flattened to a bigger circle. Wait for about 2 min and carefully remove the 2nd slide, trying not to disturb the agarose droplet. The agarose pad is ready to use in about 5 min.

9. Micropipettes (1–20 μL , 20–200 μL , 200–1000 μL) and tips
10. 1.5 mL microcentrifuge tubes
11. 15 mL plastic conical tubes
12. Glass tubes for bacterial cultures
13. Glass conical flasks for bacterial cultures
14. Whatman paper
15. Nitrocellulose membrane (0.45 or 0.2 μm)

2.2 Equipment

1. Stereomicroscope (e.g., Nikon SMZ 745)
2. Fluorescent microscope (e.g., EVOS FV Auto 2 Imaging System—ThermoFisher Scientific)
3. Standard table-top centrifuge
4. Refrigerated centrifuge
5. Power supply, vertical electrophoresis system and blotting systems (e.g., Mini-PROTEAN[®] Tetra Vertical Electrophoresis Cell, 4-gel, for 1.0 mm thick handcast gels, with Mini Trans-Blot[®] Module, Bio-Rad)
6. Laboratory shaker or rocker
7. Chemiluminescence developing system (e.g., Chemidoc Imaging System, Bio-Rad)

2.3 Reagents

A. Reagents for bacterial cultures

1. Luria-Bertani (LB) liquid medium: To prepare 1 L of liquid LB, dissolve 10 g sodium chloride (NaCl), 10 g Tryptone and 5 g yeast extract in approximately 900 mL of distilled water (H_2O). Stir the mix until it is completely dissolved. Adjust the pH to 7.0 with 5 N sodium hydroxide (NaOH), and bring the volume to 1 L with H_2O . Sterilize by autoclaving.
2. Luria-Bertani (LB) solid medium: To prepare 1 L of solid LB, follow the aforementioned recipe for liquid LB, but also add 15 g agar. The powder will not dissolve completely, as agar is only dissolved after autoclaving. Sterilize by autoclaving and wait until the medium is cooled enough (approximately 50 °C). At this step, before dispensing the medium to petri plates [approximately 18 mL per plate (92 \times 16 mm)], you can add antibiotics if needed.

B. Reagents for nematode growth and maintenance

1. Nematode Growth Media (NGM): To prepare 1 L of NGM, dissolve 3 g NaCl, 2.5 g bactopectone, 17 g agar and 0.2 g streptomycin in approximately 800 mL of distilled H_2O . Sterilize by autoclaving. After the solution has cooled down, add

1 mL of 1 M calcium chloride (CaCl_2), 1 mL of 1 M MgSO_4 , 25 mL of 1 M potassium phosphate (KPO_4), 1 mL of cholesterol (5 mg/mL in 100% ethanol) and 1 mL Nystatin (10 mg/mL in 70% ethanol). All the solutions, except for cholesterol and Nystatin, need to be sterilized by autoclaving. Bring the volume to 1 L with distilled H_2O , and after 5–10 min of stirring, pour the solution to petri plates. For the 60×15 mm plates dispense 7–8 mL of the NGM solution to each plate.

2. M9 Minimal Medium Buffer: Dissolve 3 g monopotassium phosphate (KH_2PO_4), 6 g disodium phosphate (Na_2HPO_4) and 5 g NaCl in 800 mL distilled H_2O . Sterilize by autoclaving. After the solution has cooled down, add 1 mL of sterile 1 M magnesium sulfate (MgSO_4), and bring the volume to 1 L with distilled water.
3. Tetramisole for anesthetizing the nematodes: To prepare 100 mM stock tetramisole solution, dissolve 0.24 g tetramisole hydrochloride powder in 10 mL M9 buffer. Keep it as a stock solution at 4°C . For the working solution, dilute the stock in M9, at a final concentration of 20 mM and keep it at room temperature (RT).
4. Bleaching solution for synchronizing nematode population: To prepare 10 mL of bleaching solution, add 1 mL of 5 N NaOH and 2 mL of 5% sodium hypochlorite (NaOCl) in 7 mL distilled H_2O .

C. Reagents for Western blot

1. $6 \times$ sample buffer: To prepare 10 mL solution, mix 3 mL Na-Tricine 1 M pH 7.8, 4.2 mL glycerol, 1.2 g SDS, 0.93 g DTT, 150 μL 10% Triton-X100 and 1.2 mg bromophenol blue. Bring the final volume to 10 mL with distilled H_2O . Aliquote per 1 mL and store at -20°C . Avoid freeze–thaw cycles. Once thawed, a vial is stable for several weeks at RT.
2. 10% SDS: Dissolve 5 g sodium dodecyl sulfate (SDS) in 50 mL distilled H_2O . Store at RT.
3. 10% APS: Dissolve 5 g ammonium persulfate (APS) in 50 mL distilled H_2O . Aliquote and store at -20°C .
4. 7.5% SDS polyacrylamide resolving gel: In a 15 mL conical tube mix 1.5 mL Tris–HCl 1.5 M pH 8.8, 1.5 mL 30% polyacrylamide, 3 mL distilled H_2O , 50 μL 10% SDS. Vortex briefly. Add 50 μL 10% APS and 5 μL Tetramethylethylenediamine (TEMED) immediately before casting the gel, as the addition of APS and TEMED will initiate the polymerization of acrylamide.
5. 5% Stacking gel: In a 15 mL conical tube mix 0.75 mL Tris–Cl 0.5 M pH 6.8, 0.45 mL polyacrylamide, 1.77 mL distilled H_2O , 30 μL 10% SDS. Vortex briefly. Add 30 μL 10% APS and 3 μL TEMED immediately before casting the gel.
6. $10 \times$ Running buffer: For 1 L add 30 g Tris-Base, 144 g glycine and 10 g SDS in 1 L distilled H_2O . To prepare a $1 \times$ working solution dilute 1:10 in distilled H_2O .

7. 1 × Transfer buffer: For 2L add 11.6 g Tris-Base, 5.8 g glycine and 0.75 mL 10% SDS in 1.6L distilled H₂O. Stir until all chemicals are dissolved. Then add 400 mL methanol and store at 4 °C until use. Transfer buffer can be reused for at least two times.
8. 10 × Tris-Buffered Saline (TBS) pH 7.6: For 1 L add 24 g Tris and 88 g NaCl in distilled H₂O. Adjust pH 7.6 with 12 N HCl.
9. 1 × Tris-Buffered Saline, 0.1% Tween-20 (TBS-T): To prepare 1 L add 100 mL 10 × TBS in 900 mL distilled H₂O. Then use a blue tip with a cut end to add 1 mL Tween-20. Stir until the detergent is dissolved.
10. Ponceau S solution: To prepare 100 mL solution, dissolve 0.5 g Ponceau S in 5 mL acetic acid. Bring the final volume to 100 mL with distilled H₂O. The solution can be reused multiple times.
11. 5% Blocking buffer: Dissolve 2 g non-fat milk powder in 40 mL 1 × TBS-T.
12. Antibodies: Primary antibodies: anti-GFP, anti-alpha tubulin and secondary HRP-conjugated antibodies.
13. Chemiluminescence detection kit.

2.4 Nematode strains

1. N2: *C. elegans* wild isolate
2. HZ589: *him-5(e1490)* V; *bpl151* [*p_{sqst-1}*:SQST-1::GFP+*unc-76(+)*]

2.5 Nematode food

OP50: Uracil auxotroph *E. coli* bacteria. For liquid OP50 bacterial culture, inoculate a single OP50 colony (grown overnight on an LB agar plate) into 50 mL of sterile liquid LB medium. Incubate for 4–5 h in a shaking incubator at 37 °C. Seed 200 μL of the OP50 culture in the middle of freshly prepared NGM plates, and let them grow overnight at RT (approximately for 16 h).

2.6 Microscopic analysis for monitoring autophagic flux using the SQST-1::GFP reporter strain

- A. Starvation treatment and preparation of the nematodes prior to microscopic observation
 1. Transfer 10 L4-staged nematodes of the HZ589 strain in 2 OP50-seeded NGM plates (10 worms per plate). Incubate the plates at 20 °C.
 2. After about 4–5 days, the plates will be full of gravid hermaphrodites of the 1st generation. Wash the plates with 2 mL of M9 buffer and collect the liquid in a sterile 1.5 mL microcentrifuge tube. The liquid will be less than 2 mL, as a portion of M9 buffer will be absorbed in the NGM plates. Leave the animals to settle with gravity for 2 min and discard the liquid. Add 500 μL of freshly made

bleaching solution. Shake by hand or vortex the solution for a few seconds. Repeat shaking/vortexing every 2 min until the worm bodies are completely dissolved. Do not bleach for more than 5 min, as the resulted eggs may not hatch. Spin the tube in a table-top centrifuge (~3000 rpm) for 30 s to pellet the released eggs. Discard carefully the supernatant, leaving 10–20 μ L and trying not to disturb the egg-pellet. Wash with 500 μ L of sterile M9 buffer and finally solubilize the egg pellet in 100 μ L of sterile M9 buffer. Dispense the egg solution to OP50—seeded plates. Leave the animals grow at 20°C.

3. After about 2.5–3 days, the plates will be full of L4-staged animals. Transfer 25–40 L4s to 4 new OP50-seeded plates (25–40 animals per plate) and incubate them overnight at 20°C.
4. After 16–18 h, the worms will be young Day 1 adults, the suitable developmental stage for the observation of SQST-1::GFP puncta in the head area of the nematodes. At this time point, gather 25–40 hermaphrodites from one plate and directly use them for microscopic observation. This will be the control sample, which contains normally fed animals.
5. Gather all the worms from the remaining three plates with approximately 2 mL of M9 and collect the liquid in a sterile microcentrifuge tube. Leave the animals to settle with gravity for 2 min and discard the liquid. Wash the worm pellet with 500 μ L of M9 and wait for 2 min until the animals settle again to the bottom. Discard the liquid and repeat the washing procedure until all bacteria are removed. Resuspend the worm pellet in 100 μ L M9 buffer and transfer the animals using a glass Pasteur pipette to unseeded NGM plates. Incubate the animals at 20°C. Collect 25–40 hermaphrodites every 3 h and observe them at the microscope. For our experiment we examined 3 h-, 6 h-, and 9 h-starved animals.

B. Sample preparation for imaging in the microscope

1. Place a 5 μ L drop of 20 mM tetramisole in the middle of a freshly made agarose pad.
2. Use an eyelash hair to transfer the worms one by one into the droplet. When the animals are transferred in the tetramisole drop, they immediately get immobilized.
3. Cover carefully with a coverslip and seal with a fingernail polish. This is an important step, since the animals should not dry out during the imaging process.
4. Observe the worms under a fluorescent microscope at 10 \times magnification. Acquire images of the head regions using GFP and brightfield channels. Heads are the ideal regions for monitoring SQST-1 expression, as clear and dense GFP puncta are visible without any background noise (autofluorescence) from the intestine or other tissues. Ignore worms that seem to be damaged (mainly due to mishandling during preparation). Ensure that all the images are taken by using exactly the same settings (exposure time, brightness, contrast, etc.). The imaging system we are using allows z-stack analysis. Particularly, it collects a series of images in different focal planes (we set upper/lower limits and desired width)

and returns a single focused image of maximal intensity. We took advantage of this feature, since SQST-1::GFP forms puncta in different layers of the nematode's head. If only a simple fluorescent imaging system is available, you can quantify directly the SQST-1 puncta by changing manually the focal plane and capture one representative image in which most of the puncta are visible.

C. Image analysis for the quantification of SQST-1::GFP puncta

For the quantification of SQST-1::GFP puncta, we use the ImageJ software (Schneider et al., 2012) and follow the subsequent steps.

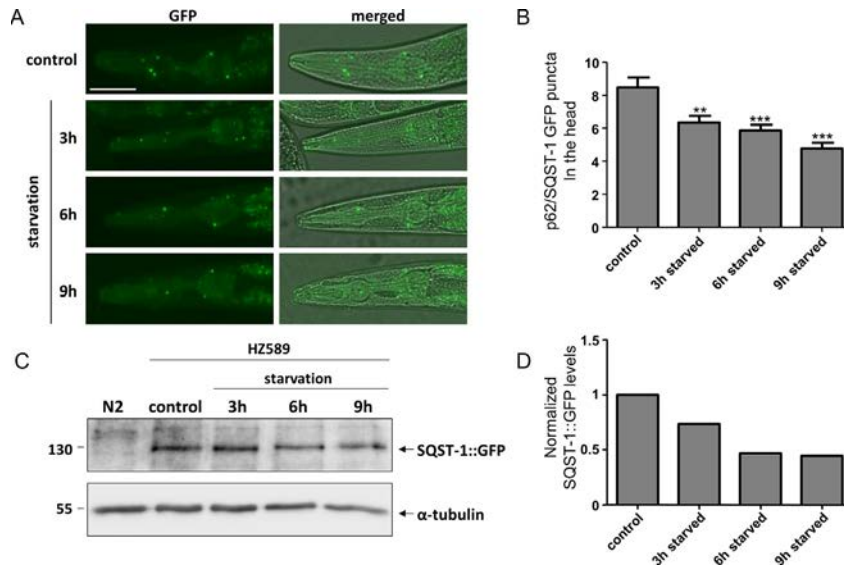
1. Open the image in ImageJ and by using a selection tool select the head region of each worm and save it in the Region of Interest (ROI) Manager. Select the entire head including both pharyngeal lobes and carefully exclude the initial part of the intestine which usually produces autofluorescence.
2. Split the channels and keep only the green one.
3. Subtract the background and set the threshold at a level where all the puncta are visible. For each selected area (saved in the ROI manager) analyze the number of puncta by running the "Analyze particles" tool.
4. Save the summary results for each sample and perform the statistical analysis using Microsoft Excel or Graphpad prism.

As shown in Fig. 1A and B, SQST-1::GFP puncta are significantly reduced under starvation, compared to the normal-feeding conditions.

2.7 Detection of SQST-1::GFP levels by western blot

The HZ589 strain can be used to monitor SQST-1::GFP protein levels by western blot analysis.

1. Following the instructions described above (section A), prepare 40–50 D1 hermaphrodite worms per experimental condition.
2. Collect worms in M9 buffer. Wash 2–3 times using 0.5–1 mL M9 buffer, until bacteria are removed. Between each wash, allow worms to settle by gravity for 3–5 min.
3. Once washing is complete, aspirate the M9 solution leaving approximately 20 μ L. Add 5 μ L sample buffer and incubate at 95 °C for 10 min. At this point samples can be stored at –20 °C. Before loading, centrifuge the samples at full speed (approximately 17,000 g) in a refrigerated centrifuge for 10 min. This step is necessary, as occasionally worms do not completely dissolve through boiling in sample buffer.
4. Prepare a 7.5% SDS-polyacrylamide gel. Place the spacer plate and the short plate in the casting frame. Add approximately 4.5 mL of the resolving gel and 1 mL of isopropanol on top. Save the remaining quantity of the resolving gel in the conical tube, to check for gel polymerization. When the resolving gel is

**FIG. 1**

Monitoring autophagic flux by using the SQST-1::GFP reporter. (A and B) Quantification of SQST-1::GFP puncta, formed in the head region of control (normally fed) and starved Day 1 adult animals ($n=30$). Quantitative results are reported as means \pm SEM. Symbols indicate statistical comparisons (one-way ANOVA followed by Tukey's multiple comparisons test) with controls (** $p < 0.01$, *** $p < 0.001$). Scale bar 50 μ m. (C and D) Total worm lysates from SQST-1::GFP control (normally fed) and starved Day 1 adult animals were immunoblotted against the indicated proteins. In the graph, SQST-1::GFP levels are normalized to alpha-tubulin and presented relative to control.

polymerized, remove the isopropanol and add the stacking gel. Place the comb to create the wells and allow polymerization to occur.

- To perform the electrophoresis, place the gel in the tank, according to the manufacturer instructions and fill with $1 \times$ Running buffer. Load the samples carefully avoiding any precipitate. Load as well a pre-stained protein marker in order to visualize the molecular weights of the proteins. Perform the electrophoresis at 70 V for 15 min and then at 100–120 V until the bromophenol blue front reaches the end of the gel.
- Proceed to the wet transfer. Cut two Whatman papers at the size of the sponges. Cut a piece of the nitrocellulose membrane at the size of the gel. Soak the papers, the sponges and the membrane in cold $1 \times$ transfer buffer. Separate the spacer and short plates to obtain the gel and remove the stacking part. To assemble the transfer cassette, place the black part on the bottom, add a sponge, a Whatman paper, the gel, the membrane, a Whatman paper and on top a sponge. Close the cassette carefully to avoid the creation of bubbles that would

impede the transfer of the proteins from the gel to the membrane. Place the transfer cassette in the electrode assembly in the tank, a self-contained ice (cooling unit) and fill with cold $1 \times$ transfer buffer. Perform the transfer at 100 V for 90 min.

7. Optionally stain the membrane with Ponceau-S solution to verify successful transfer of the proteins. To this end, incubate the membrane with Ponceau-S solution for a few minutes in a Tupperware on a shaker. Then wash the membrane using distilled H₂O or TBS-T, until the protein bands are detectable. Taking into account that the SQST-1::GFP fusion protein runs approximately at 130 kDa and the loading control alpha-tubulin at 55 kDa, the membrane can be horizontally cut at half, to immunoblot in parallel both proteins. Perform additional washes to completely de-stain the Ponceau-S stain.
8. Incubate the membrane with blocking solution for 1 h at RT shaking.
9. Dilute the primary antibodies in blocking buffer, according to the data sheet. Incubate the membrane with the diluted antibodies overnight at 4 °C on a shaker. To reduce the amount of antibody used, place the membrane in a zip-lock bag and seal.
10. The following day perform three washes of the membrane with TBS-T, for 10 min on a shaker.
11. Incubate the membrane with the HRP-conjugated secondary antibody, diluted in blocking solution according to the datasheet, for 1 h at RT on a shaker.
12. Wash the membrane three times with TBS-T.
13. Add the chemiluminescence substrate on the membrane according to the datasheet and develop the membrane using a digital developing system, such as the Chemidoc Imaging System (Bio-Rad), or a film.
14. Perform densitometry analysis using the Image J software, to quantify the protein levels of SQST-1::GFP and normalize to the loading control alpha-tubulin.

As shown in Fig. 1C and D, starvation results in the reduction of SQST-1::GFP protein levels, compared to the normal-feeding conditions.

2.8 Notes

1. The method described here should always be used in combination with the analysis of LGG-1 expression for the accurate monitoring of autophagic flux.
2. Exposure to tetramisole, the anesthetizing agent used during sample preparation, has been shown to increase the number of GFP::LGG-1 puncta and induce HLH-30/TFEB nuclearization (Lapierre et al., 2013; Zhang et al., 2015). However, even 30 min exposure to tetramisole does not alter the levels of p62/SQST-1 puncta (Fig. 2). Alternatively, another commonly used anesthetic drug is sodium azide (NaN₃). However, since it is known that sodium azide perturbs mitochondrial homeostasis, it should be avoided in mitochondria-related studies (Bogucka & Wojtczak, 1966). Irrespectively of the type of anesthetic

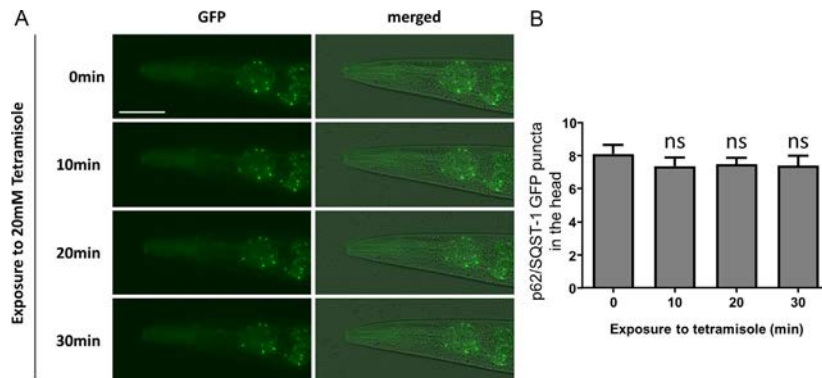


FIG. 2

Assessing the effect of tetramisole as an anesthetic drug, in the expression pattern of the SQST-1::GFP reporter. (A and B) Quantification of SQST-1::GFP puncta, formed in the head region of Day 1 adult animals ($n=30$), mounted in 20mM tetramisole supplemented agarose pads. Images of the same slide were captured every 10min for 30min in total. Quantitative results are reported as means \pm SEM. Symbols indicate statistical comparisons (one-way ANOVA followed by Tukey's multiple comparisons test) with controls (ns, no statistical significance). Scale bar 50 μ m.

Table 1 Commonly used genetic/pharmacological manipulations that induce or block autophagy.

	Manipulation	Effect on autophagy	Indicative References
Genetic interventions	<i>daf-2(RNAi)</i> or cross with <i>daf-2(e1370)</i> mutants	Induction	Hansen et al. (2008) and Chang et al. (2017)
	Cross with <i>eat-2(ad465)</i> mutants	Induction	Hansen et al. (2008)
	<i>bec-1(RNAi)</i>	Inhibition	Samara, Syntichaki, and Tavernarakis (2008)
	<i>unc-51(RNAi)</i>	Inhibition	Kumsta et al. (2017)
Chemical compounds	<i>lgg-1(RNAi)</i>	Inhibition	Samara et al. (2008)
	Rapamycin	Induction	Feleciano et al. (2019)
	Spermidine	Induction	Eisenberg et al. (2009)
	Resveratrol	Induction	Morselli et al. (2010)
	Bafilomycin-A1	Inhibition	Kumsta et al. (2019)
	Chloroquine	Inhibition	Chapin et al. (2015)
	Wortmannin	Inhibition	Samokhvalov, Scott, and Crowder (2008)
	3-Methyladenine	Inhibition	Samokhvalov et al. (2008)

used, it is highly recommended to prepare each sample just before microscopic observation and ensure that all conditions are imaged within the same time window.

3. Use only hermaphrodites for microscopy and western blot analysis. HZ589 is a *him* mutant strain and produces many males at each generation.
4. Animals should be well fed (not starved) for at least three generations before using them for experiments.

3 Concluding remarks

The current protocol provides a detailed description of two methodological approaches, to assess SQST-1 protein levels in *C. elegans*. The fluorescent imaging analysis serves as a rapid and relatively easy method to measure the *in vivo* levels of SQST-1. In parallel, the western blot analysis may be used as an independent read-out to further validate the experimental findings. Analysis of SQST-1 levels can be performed under various pharmacological treatments, upon genetic crossing with mutant strains or other fluorescent reporters, as well as in unbiased RNAi screens. In [Table 1](#) we summarize genetic and pharmacological manipulations that are commonly used to induce or block autophagy in *C. elegans* and could serve as positive and negative controls. The precise monitoring of the autophagic flux under various experimental conditions will provide critical insight on the molecular mechanisms of autophagy and its prominent role in health and disease.

Acknowledgments

We thank A. Pasparaki for expert technical support. Nematode strains used in this work were provided by the *Caenorhabditis* Genetics Center, which is funded by the National Centre for Research Resources of the National Institutes of Health, and S. Mitani (National Bioresource Project) in Japan. We thank A. Fire for plasmid vectors. This work was supported by grants from the European Research Council (ERC-GA695190-MANNA) and the project “BIOIMAGING-GR” (MIS5002755), which is implemented under the Action “Reinforcement of the Research and Innovation Infrastructure,” funded by the Operational Programme “Competitiveness, Entrepreneurship and Innovation” (NSRF 2014–2020) and co-financed by Greece and the European Union (European Regional Development Fund).

References

- Aspernig, H., et al. (2019). Mitochondrial perturbations couple mTORC2 to autophagy in *C. elegans*. *Cell Reports*, 29(6), 1399–1409. (e5).
- Bogucka, K., & Wojtczak, L. (1966). Effect of sodium azide on oxidation and phosphorylation processes in rat-liver mitochondria. *Biochimica et Biophysica Acta (BBA) - Enzymology and Biological Oxidation*, 122(3), 381–392.

- Chang, J. T., et al. (2017). Spatiotemporal regulation of autophagy during *Caenorhabditis elegans* aging. *eLife*, 6, e18459.
- Chapin, H. C., et al. (2015). Tissue-specific autophagy responses to aging and stress in *C. elegans*. *Aging (Albany NY)*, 7(6), 419–434.
- Champilas, N., et al. (2020). Acyl-CoA-binding protein (ACBP): A phylogenetically conserved appetite stimulator. *Cell Death & Disease*, 11(1), 7.
- Chen, Y., Scarcelli, V., & Legouis, R. (2017). Approaches for studying autophagy in *Caenorhabditis elegans*. *Cells*, 6(3), 27.
- Dikic, I., & Elazar, Z. (2018). Mechanism and medical implications of mammalian autophagy. *Nature Reviews. Molecular Cell Biology*, 19(6), 349–364.
- Eisenberg, T., et al. (2009). Induction of autophagy by spermidine promotes longevity. *Nature Cell Biology*, 11(11), 1305–1314.
- Fang, E. F., et al. (2019). Mitophagy inhibits amyloid-beta and tau pathology and reverses cognitive deficits in models of Alzheimer's disease. *Nature Neuroscience*, 22(3), 401–412.
- Feliciano, D. R., et al. (2019). Crosstalk between chaperone-mediated protein disaggregation and proteolytic pathways in aging and disease. *Frontiers in Aging Neuroscience*, 11, 9.
- Feng, Y., et al. (2014). The machinery of macroautophagy. *Cell Research*, 24(1), 24–41.
- Galluzzi, L., et al. (2017). Pharmacological modulation of autophagy: Therapeutic potential and persisting obstacles. *Nature Reviews. Drug Discovery*, 16(7), 487–511.
- Guerrero-Gomez, D., et al. (2019). Loss of glutathione redox homeostasis impairs proteostasis by inhibiting autophagy-dependent protein degradation. *Cell Death and Differentiation*, 26(9), 1545–1565.
- Guo, B., et al. (2014). The nascent polypeptide-associated complex is essential for autophagic flux. *Autophagy*, 10(10), 1738–1748.
- Hansen, M., et al. (2008). A role for autophagy in the extension of lifespan by dietary restriction in *C. elegans*. *PLoS Genet*, 4(2), 0040024.
- Kalfalah, F., et al. (2016). Crosstalk of clock gene expression and autophagy in aging. *Aging (Albany NY)*, 8(9), 1876–1895.
- Kaushik, S., & Cuervo, A. M. (2018). The coming of age of chaperone-mediated autophagy. *Nature Reviews. Molecular Cell Biology*, 19(6), 365–381.
- Kim, H., et al. (2018). The small GTPase RAC1/CED-10 is essential in maintaining dopaminergic neuron function and survival against alpha-Synuclein-induced toxicity. *Molecular Neurobiology*, 55(9), 7533–7552.
- Klionsky, D. J., et al. (2016). Guidelines for the use and interpretation of assays for monitoring autophagy (3rd edition). *Autophagy*, 12(1), 1–222.
- Kovács, A. L. (2015). The application of traditional transmission electron microscopy for autophagy research in *Caenorhabditis elegans*. *Biophysics Reports*, 1, 99–105.
- Kumsta, C., et al. (2017). Hormetic heat stress and HSF-1 induce autophagy to improve survival and proteostasis in *C. elegans*. *Nature Communications*, 8(1), 14337.
- Kumsta, C., et al. (2019). The autophagy receptor p62/SQST-1 promotes proteostasis and longevity in *C. elegans* by inducing autophagy. *Nature Communications*, 10(1), 5648.
- Kyriakakis, E., Markaki, M., & Tavernarakis, N. (2015). *Caenorhabditis elegans* as a model for cancer research. *Molecular & Cellular Oncology*, 2(2), e975027.
- Lapierre, L. R., et al. (2013). The TFEB orthologue HLH-30 regulates autophagy and modulates longevity in *Caenorhabditis elegans*. *Nature Communications*, 4, 2267.
- Levine, B., & Kroemer, G. (2008). Autophagy in the pathogenesis of disease. *Cell*, 132(1), 27–42.

- Levy, J. M. M., Towers, C. G., & Thorburn, A. (2017). Targeting autophagy in cancer. *Nature Reviews. Cancer*, *17*(9), 528–542.
- Markaki, M., Palikaras, K., & Tavernarakis, N. (2018). Novel insights into the anti-aging role of Mitophagy. *International Review of Cell and Molecular Biology*, *340*, 169–208.
- Menzies, F. M., et al. (2017). Autophagy and neurodegeneration: Pathogenic mechanisms and therapeutic opportunities. *Neuron*, *93*(5), 1015–1034.
- Metaxakis, A., Ploumi, C., & Tavernarakis, N. (2018). Autophagy in age-associated neurodegeneration. *Cells*, *7*(5), 37.
- Morselli, E., et al. (2010). Caloric restriction and resveratrol promote longevity through the Sirtuin-1-dependent induction of autophagy. *Cell Death & Disease*, *1*(1), e10. <https://doi.org/10.1038/cddis.2009.8>.
- Oku, M., & Sakai, Y. (2018). Three distinct types of microautophagy based on membrane dynamics and molecular machineries. *BioEssays*, *40*(6), 1800008.
- Palmisano, N. J., & Melendez, A. (2016a). Detection of autophagy in *Caenorhabditis elegans* using GFP::LGG-1 as an autophagy marker. *Cold Spring Harbor Protocols*, *2016*(1), pdb prot086496.
- Palmisano, N. J., & Melendez, A. (2016b). Detection of autophagy in *Caenorhabditis elegans* by Western blotting analysis of LGG-1. *Cold Spring Harbor Protocols*, *2016*(2), pdb prot086512.
- Pankiv, S., et al. (2007). p62/SQSTM1 binds directly to Atg8/LC3 to facilitate degradation of ubiquitinated protein aggregates by autophagy. *The Journal of Biological Chemistry*, *282*(33), 24131–24145.
- Papandreou, M. E., & Tavernarakis, N. (2017). Monitoring autophagic responses in *Caenorhabditis elegans*. *Methods in Enzymology*, *588*, 429–444.
- Pietrocola, F., et al. (2018). Aspirin recapitulates features of caloric restriction. *Cell Reports*, *22*(9), 2395–2407.
- Reggiori, F., et al. (2012). Autophagy: More than a nonselective pathway. *International Journal of Cell Biology*, *2012*, 219625.
- Saha, S., et al. (2018). Autophagy in health and disease: A comprehensive review. *Biomedicine & Pharmacotherapy*, *104*, 485–495.
- Samara, C., Syntichaki, P., & Tavernarakis, N. (2008). Autophagy is required for necrotic cell death in *Caenorhabditis elegans*. *Cell Death & Differentiation*, *15*(1), 105–112.
- Samokhvalov, V., Scott, B. A., & Crowder, C. M. (2008). Autophagy protects against hypoxic injury in *C. elegans*. *Autophagy*, *4*(8), 1034–1041.
- Schneider, C., et al. (2012). NIH Image to ImageJ: 25 years of image analysis. *Nature Methods*, *9*(7), 671–675.
- Scott, T. A., et al. (2017). Host-microbe co-metabolism dictates Cancer drug efficacy in *C. elegans*. *Cell*, *169*(3), 442–456. (e18).
- Sharma, M., Pandey, R., & Saluja, D. (2018). ROS is the major player in regulating altered autophagy and lifespan in *sin-3* mutants of *C. elegans*. *Autophagy*, *14*(7), 1239–1255.
- Tian, Y., et al. (2010). *C. elegans* screen identifies autophagy genes specific to multicellular organisms. *Cell*, *141*(6), 1042–1055.
- Wong, S. Q., et al. (2020). *C. elegans* to model autophagy-related human disorders. *Progress in Molecular Biology and Translational Science*, *172*, 325–373.
- Zhang, H., et al. (2015). Guidelines for monitoring autophagy in *Caenorhabditis elegans*. *Autophagy*, *11*(1), 9–27.
- Zhou, Y., et al. (2019). A secreted microRNA disrupts autophagy in distinct tissues of *Caenorhabditis elegans* upon ageing. *Nature Communications*, *10*(1), 4827.